Indian Journal of Fibre & Textile Research
Vol. 51, June 2026, pp. 176-186
DOI: 10.56042/ijftr.v51i2.21823

Influence of fly ash and abaca fibre reinforcement on the mechanical and physical properties of polypropylene composites

Ravindra Gode[1], Vivek Gaval[2,a] & Dattatraya kakad[3]

[1]Department of Engineering Science, Dr. D.Y. Patil Deemed to be University, Navi Mumbai 400 706, India
[2]Department of General Engineering, Institute of Chemical Technology, Mumbai 400 019, India
[3]Department of Textile Engineering, Veermata Jijabai Technological Institute, Mumbai 400 019, India

Received 21 January 2025; revised received and accepted 13 January 2026

The growing demand for sustainable and high-performance materials has sparked significant interest in hybrid composites that incorporate natural fibres and industrial waste products. This study focuses on the fabrication and evaluation of polypropylene (PP) composites reinforced with *abaca* (*Musa textilis*) fibres and fly ash (FA) as a filler, with and without a compatibilizer. Composite samples were fabricated with different fibre contents while keeping the FA loading constant. Standard ASTM dimensions were used for preparing the specimens required for experimental testing. Mechanical and physical properties, including tensile, flexural, impact strength, hardness, density, water absorption, and void content, were systematically evaluated. Field Emission Scanning Electron Microscopy (FESEM) analysis of the tensile fracture surfaces revealed that the addition of a compatibilizer improved the fibre–matrix interfacial adhesion and reduced the number of voids. The results demonstrated that composites with 7.5–10 wt.% abaca fibre and 3 wt.% compatibilizer exhibited optimal performance. This study provided the potential of abaca fibre and FA-based PP composites as lightweight, supportive sustainable material for applications in automotive, packaging, and consumer products.

Keywords: Abaca fibre, FESEM, Fly Ash, Hybrid composites, Mechanical properties, Polypropylene, Sustainable material

1 Introduction

Polypropylene composites reinforced with natural fibres have gained considerable interest due to their favourable mechanical properties, low density, and environmental benefits. The performance of natural fibre composites depends on factors such as fibre type, chemical compatibility, and processing techniques. Bast fibres, generally showed superior stiffness and strength due to their high cellulose content. Surface treatments such as alkali and silane were reported to enhance fibre–matrix adhesion and reduce moisture sensitivity. Manufacturing processes significantly influenced fibre dispersion and porosity control, supporting the viability of natural fibres as alternatives to glass fibres in lightweight applications[1]. Recent reviews further highlighted advances in processing and hybridization strategies. These studies emphasized the need for careful selection of fibre and filler loadings to achieve processing-compatible and high-performance PP hybrids[2].

The alkali treatment of abaca fibres improved crystallinity and tensile strength by removing hemi cellulose and promoting molecular alignment. The duration of treatment was found to be critical and optimal times lead to improved reinforcement performance[3]. Abaca fibre exhibited a higher tensile strength ranging from 400 to 980 MPa than many other natural fibres, demonstrated potential for structural and automotive applications while chemical treatments such as alkali and silane reduced moisture sensitivity and enhanced fibre–matrix interaction[2,4, 5].

The application of abaca fibres is strengthened by their high tensile strength, compatibility in hybrid systems, and environmental sustainability. Chemical modifications and hybridization with synthetic fibres were highlighted as effective methods to improve mechanical performance[6]. Studies on chemically treated abaca fibre composites showed that alkali and diazonium modifications significantly enhanced tensile properties with an optimal fibre loading of 40 wt.% was identified, while higher loadings lead to agglomeration and poor dispersion[7]. Statistical models have also been used to analyze abaca fibre strength. These studies reported tensile strength values between 100 and 900 MPa and showed that a log-normal distribution effectively represents natural variability. A screening method was proposed to

[a]Corresponding author.
E-mail: vr.gaval@ictmumbai.edu.in

minimize property variations in structural applications[8].

Hybrid composites reinforced with abaca, banana, and glass fibres demonstrated improved tensile, flexural, and impact performance compared to single-fibre composites. The combination of abaca for stiffness and glass/banana for toughness resulted in a balanced mechanical response[9]. Natural synthetic hybrid fibre composites also showed improvements in strength, stiffness, and durability, however, issues related to consistency and cost-effectiveness at industrial scales remain[10]. Recent worked on abaca-specific PP composites provides updated experimental benchmarks for tensile and flexural properties and supports the used of moderate fibre loadings in thermoplastic matrices[11].

Functionalization of polylactic acid with maleic anhydride improved compatibility with natural fibres. Maleic anhydride-grafted-polylactic acid enhanced fibre–matrix bonding, reduced voids, and improved thermal and mechanical properties, demonstrating its efficacy as a coupling agent[12]. PP/EPDM blends modified with graphene oxide and polypropylene-grafted-maleic anhydride (PP-g-MA) also showed improved tensile strength, elongation, modulus, and thermal stability while microstructural analysis confirmed finer phase dispersion and stronger interfacial bonding[13].

Fly ash is a sustainable and low-cost filler due to its high surface area and aluminosilicate composition, demonstrating effectiveness in various applications such as cement, geopolymers, and polymer composites by enhancing mechanical and thermal properties[14]. The flax fibre-reinforced PP composites containing 0–10 wt.% lignite FA, observed that at 5 wt.% FA increased wear resistance, surface hydrophobicity, and thermal stability, while compressive strength and crystallinity improved with increasing FA content[5]. Studies on sisal-FA-PP composites showed good recyclability, with 15 wt.% FA retained more than 95% of their original tensile and flexural strength after recycling. Additional reinforcement with 5 wt.% sisal contributed to improved mechanical recovery, highlighting the stabilizing effect of FA[15]. Experiments using untreated and surface-treated FA in PP composites revealed that surface-modified FA significantly improved interfacial bonding, tensile strength, and thermal stability, whereas untreated FA resulted in poor dispersion and diminished performance[16].

Recent research on industrial waste fillers confirmed that FA enhanced stiffness, wear resistance and thermal stability at low-to-moderate loadings. Fly-ash–filled polyolefin composites showed notable enhancements at 5–15 wt.% filler levels, with morphological evidence linking particle dispersion to property changes[17]. Recent reviews and experimental studies also underlined that the importance of compatibilization and surface functionalization of FA. Chemically active or surface-modified FA at 5 wt.% can significantly improve matrix–particle adhesion and thermal performance[18].Combining PP fibres with FA enhanced strength and durability through micro-filling effects and improved interfacial bonding. These mechanisms also relevant to fibre–FA hybrid polymer composites[19].

Multiple studies have consistently showed that adding 5–10 wt.% FA in natural fibre-reinforced PP composites enhanced mechanical strength, wear resistance, and thermal stability. Based on the literature, FA content in the present work was fixed at 10 wt.%. Higher FA levels may lead to particulate clustering and reduced mechanical integrity, whereas lower additions at 5 wt.% provide limited enhancement. This selected range provides a balanced combination of mechanical and processing performance. The improvements are primarily attributed to increased crystallinity and improved fibre–matrix interface morphology, with tensile and flexural properties remaining stable even after recycling.

Abaca fibre was used in the range of 2.5–10 wt.% in this study. This range was selected because low to moderate fibre loadings in PP generally provide effective reinforcement without causing fibre agglomeration or insufficient matrix wetting. Previous studies on lignocellulosic fibres showed that loadings above 10 wt.% often reduce processability and lead to weak interfacial bonding. The selected range therefore enables evaluation of the lower and upper limits of fibre contribution while maintaining stable melt flow during compounding and molding.

Although numerous studies have examined natural fibre and FA-reinforced PP composites, limited research has focused specifically on the use of abaca fibre in combination with FA in PP matrices. The present study fills this gap by developing PP-based hybrid composites reinforced with abaca fibre and FA. This work embodies a transdisciplinary methodology intersecting materials science, and

environmental engineering, thereby supporting the advancement of sustainable material systems through holistic, cross-sector innovation.

2 Materials and Methods

2.1 Resources

The polymer matrix used in this study was polypropylene of grade H110MA, obtained from Reliance Industries Limited (Gujarat, India). It exhibited a melt flow index (MFI) of 11 g/10 min and a density of 0.9 g/cm³. The reinforcement material, raw abaca fibres, was sourced from the fibre Region (Chennai, India). As per supplier data and corroborated literature, the chemical composition of abaca includes 76.6% cellulose, 14.6% hemicellulose, 8.4% lignin, 0.3% pectin, and 0.1% waxes and fats. The fibres possessed a density of approximately 1.5 g/cm³, consistent with commonly reported values in literature[20]. The fibre thickness varied between 1 and 5 mm, and the tensile strength ranged from 72.59 to 148.93 MPa. Strain rates during tensile testing ranged from 0.0102 to 0.0199 mm/min, indicating moderate extensibility, making the fibres suitable for semi-structural reinforcement applications[20].

For processing, the abaca fibres were initially rinsed with distilled water to remove surface impurities and sun-dried for 360 h. They were subsequently cut to 2–3 mm lengths using a gardener's cutter, sieved for size uniformity, and stored in airtight containers to minimize moisture absorption. Before melt blending, the fibres were air-dried at room temperature for 24 h and oven-dried at 70 °C for 1 h to eliminate residual moisture and enhance matrix compatibility.

Class F fly ash, used as a secondary filler, was collected from a thermal power plant in Nagpur, India. It exhibited a density of 1.0 g/cm³ and an average particle size of 90 µm. It is a pozzolanic material generated from the combustion of anthracite or bituminous coal, with the combined content of SiO_2, Al_2O_3, and Fe_2O_3 typically exceeding 70%, supporting its classification as a predominantly siliceous filler[21, 22].

A commercial-grade polypropylene-grafted maleic anhydride (PP-g-MAH) compatibilizer was sourced from Pluss Advanced Technologies (Haryana, India). It was incorporated at varying concentrations (0–3 wt.%) to enhance interfacial adhesion between the hydrophilic abaca fibres and the hydrophobic PP matrix. The compatibilizer contains maleic anhydride functional groups grafted onto the PP backbone, which promote chemical interaction and improve stress transfer efficiency, as shown in Fig. 1. PP-g-MAH has been widely reported to improve fibre–matrix interaction and stress transfer in natural fibre-reinforced thermoplastics.

2.2 Composite Preparation

The composite constituents were proportioned according to the weight fractions outlined in Table 1. Initially, mechanical pre-mixing was performed using a mechanical stirrer (Model 9000, ICT Mumbai) operated at 80 rpm for 10 minutes, ensuring a uniform preliminary distribution of the fibres and fillers [20, 24].

As shown in Fig. 2, the homogenized blend was subsequently fed into a co-rotating twin-screw extruder (Model Lab-20, ICT Mumbai), equipped with a screw diameter of 22 mm, a length-to-diameter (L/D) ratio of 22:1, and operated at a screw speed of 26 rpm. The extrusion process was carried out through four controlled heating zones set to 180 °C, 190 °C, 200 °C, and 215 °C, with the die temperature maintained at 230 °C to ensure uniform melt flow and proper dispersion of fibres and FA within the PP matrix.

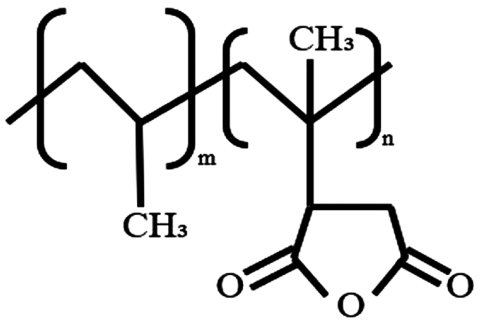

Fig. 1 — Possible Chemical Structure of PP-g-MAH[23]

Table 1 — Composite Formulations

Composite Specimens	PP, wt. %	FA, wt. %	Abaca Fibre, wt.%	Compatibilizer, wt.%
AB2.5FA10C0	87.5	10	2.5	0
AB5.0FA10C0	85.0	10	5.0	0
AB7.5FA10C0	82.5	10	7.5	0
AB10FA10C0	80.0	10	10	0
AB2.5FA10C2	85.5	10	2.5	2
AB5.0FA10C2	83.0	10	5.0	2
AB7.5FA10C3	79.5	10	7.5	3
AB10FA10C3	77.0	10	10	3
FA10	90.0	10	0	0
PP100	100	0	0	0

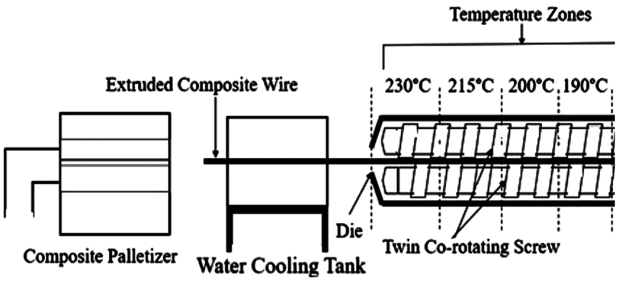

Fig. 2 — Twin Screw Extrusion with Temperature Zones

The resulting extrudate was granulated using a rotary pelletizer (Model 160) at 80 rpm, followed by oven drying at 60–70 °C for 2 h to remove any residual moisture before molding.

The dried pellets were converted into standard test specimens using an injection molding machine (Model PST 30, ICT Mumbai), following the dimensional requirements of ASTM standards for mechanical characterization. The injection molding was carried out in four temperature zones set at 230 °C, 230 °C, 255 °C, and 260 °C, respectively, while maintaining an oil temperature of 55 °C to ensure consistent melt temperature and dimensional stability of molded parts.

2.3 Characterization of Fabricated Specimens

Physical testing was performed to determine the density, water absorption, and void content of the composites. Standard laboratory conditions and ASTM-specified methods were followed, and results represent the average of five specimens.

2.3.1 Water Absorption

Water absorption was measured according to ASTM D570. Specimens (50 × 10 × 10 mm) were oven-dried at 50 °C for 1 h, cooled, and weighed (W_d). Samples were then immersed in distilled water at room temperature for 24 hours, removed, blotted dry, and reweighed (W_w). Water absorption (%) was calculated using:

$$WaterAbsorption(\%) = \frac{W_w - W_d}{W_d} \times 100 \quad \text{... (1)}$$

2.3.2 Density

Density was determined using Archimedes' principle under ASTM D792. Rectangular specimens (10 × 10 × 3 mm) were weighed in air (W_{air}) and submerged in water (W_{water}). The experimental density (ρ_{exp}) was calculated as:

$$\rho_{exp} = \frac{W_{air}}{W_{air} - W_{water}} \times \rho_{water} \quad \text{...(2)}$$

To further assess lightweight efficiency, the specific density of the composites was calculated as the ratio of the composite density to the density of water (1.0 g/cm³) and it is dimensionless.

2.3.3 Void Content

Void content was evaluated per ASTM D2734. The theoretical density (ρ_{theo}) was calculated using the rule of mixtures:

$$\rho_{theo} = \frac{1}{\frac{W_f}{\rho_f} + \frac{W_a}{\rho_a} + \frac{W_p}{\rho_p}} \quad \text{...(3)}$$

The void content (%) was then determined using:

$$Void\ Content\ (\%) = \left(\frac{\rho_{theo} - \rho_{exp}}{\rho_{theo}}\right) \times 100 \quad \text{…(4)}$$

where W_f, W_a, and W_p are the weight fractions of the fibre, FA, and PP, respectively, and ρ_f, ρ_a, and ρ_p are their densities.

2.4 Mechanical Testing of Fabricated Composites

Mechanical testing was conducted to evaluate the strength, stiffness, and toughness properties of the fabricated composite specimens. All tests were performed under standard laboratory conditions using calibrated equipment. The tests were performed following ASTM standards, and the average values of five specimens were reported for each composition.

2.4.1 Tensile Testing

The tensile properties, including tensile strength, tensile modulus, and elongation at break, were evaluated per ASTM D638 using a universal testing machine (UTM) (model no. 0511, Institute of Chemical Technology (ICT), Mumbai, Maharashtra, India) equipped with a 0-500 kg load capacity. The specimens were prepared in a Type I dog-bone geometry, with a gauge length of 50 mm. The tests were conducted at a crosshead speed of 50 mm/min and a travel limit of 800 mm. This test measured the resistance of the composite to axial tensile forces, providing insights into the fibre-matrix interfacial bonding, stiffness, and deformability of the material under load.

2.4.2 Flexural Testing

Flexural properties were evaluated using a UTM (Model 1003, Veermata Jijabai Technological Institute, Mumbai, Maharashtra, India) following ASTM D790 standards. Test was performed under three-point bending method, with specimens measuring 130 mm x 12.7 mm x 6 mm, a span length

of 60 mm, a travel limit until fracture, a load capacity of 0–250 kg and a crosshead speed of 2 mm/min, these tests assessed the material's ability to resist bending stresses and determine its flexural modulus and strength.

The flexural modulus was recorded from the machine data and flexural strength (σ_f) were calculated by using the following equation in the units of MPa.

$$\sigma_f = \frac{3FL}{2bd^2} \quad ...(5)$$

where F is the applied load at the deflection point, L is the span length, b and d are the width and thickness of the specimen, respectively.

2.4.3 IZOD Impact Testing

Impact strength was measured using a notched IZOD test (Model 174, Institute of Chemical Technology, Mumbai, Maharashtra, India) as per ASTM D256. Test specimens were prepared by measuring dimensions 63 mm × 12 mm × 12 mm, with a notch depth of 2.54. The test was performed using a pendulum impact tester. This test revealed the toughness of the composite and the effect of fibre and filler dispersion under sudden loading.

2.4.4 Shore D Hardness testing

The Shore D hardness of the fabricated composite specimens was measured according to ASTM D2240 using a digital Shore D durometer (Model 380, Institute of Chemical Technology, Mumbai, Maharashtra, India). Specimens were prepared with flat and smooth surfaces, having minimum dimensions of 60 mm x 12.7 mm x 6 mm, as recommended by the standard. Measurements were taken by applying the indenter perpendicularly to the specimen surface under a consistent force. This test provided insights into the surface resistance and rigidity of the composites.

2.4.5 Surface and Structure Analysis

FESEM was employed to analyze the surface morphology and microstructural characteristics of the fractured surfaces of the composite specimens. This technique was crucial for understanding the fibre–matrix interfacial bonding, fibre dispersion, FA distribution, and failure mechanisms in the hybrid composites. Tensile test specimens that fractured during ASTM D638 testing were selected for FESEM analysis[23] The fractured edges were carefully cut into small pieces (approximately 10 mm x 10 mm) and mounted on FESEM stubs using conductive carbon tape. The samples were gold-coated using a sputter coater (Model 098, Indian Institute of Technology, Mumbai, Maharashtra, India) before examination under the FESEM to avoid charging during imaging. The analysis was conducted using a FESEM (Model 300, Zeiss Gemini, Indian Institute of Technology, Mumbai, Maharashtra, India), operated at anaccelerating voltage of 10–20 kV depending on the required resolution. FESEM analysis helped to assess the dispersion of natural fibres and FA particles within the PP matrix, to observe pull-out or breakage of fibres, and identify the nature of failure (adhesive or cohesive), to detect voids, cracks, or agglomeration that could explain variations in mechanical properties, to evaluate the effectiveness of alkali treatment and compatibilizer (PP-g-MAH) in improving interfacial bonding. FESEM images were recorded at 250× magnification, which provided clear visualization of the fracture morphology.

3 Results and Discussion

3.1 Physical Properties

The physical properties of the fabricated composites, including density, void content, and water absorption, are listed in Table 2.

The highest density (1.922 ± 0.07 g/cm³) was recorded for the sample with 10 wt.% abaca fibre and

Table 2 — Physical Properties of Fabricated Composite Specimens: Mean and Standard Deviations (SD)

Composite Specimens	Density ± SD, g/cm³	Specific Density ± SD, g/cm³	Water Absorption ± SD, %	Void Content ± SD, %
AB2.5FA10C0	1.298 ± 0.07	1.298 ± 0.07	0.102 ± 0.08	0.15 ± 0.06
AB5.0FA10C0	1.506 ± 0.05	1.506 ± 0.05	0.101 ± 0.02	0.16 ± 0.03
AB7.5FA10C0	1.714 ± 0.14	1.714 ± 0.14	0.101 ± 0.03	0.16 ± 0.07
AB10FA10C0	1.922 ± 0.07	1.922 ± 0.07	0.101 ± 0.01	0.32 ± 0.04
AB2.5FA10C2	1.276 ± 0.07	1.276 ± 0.07	0.103 ± 0.00	0.16 ± 0.03
AB5.0FA10C2	1.484 ± 0.05	1.484 ± 0.05	0.000 ± 0.00	0.16 ± 0.02
AB7.5FA10C3	1.681 ± 0.06	1.681 ± 0.06	0.100 ± 0.07	0.31 ± 0.06
AB10FA10C3	1.889 ± 0.02	1.889 ± 0.02	0.107 ± 0.02	0.32 ± 0.01
FA10	1.076 ± 0.02	1.076 ± 0.02	0.103 ± 0.01	0.18 ± 0.01
PP100	0.9 ± 0.01	0.9 ± 0.01	0.1 ± 0.00	0.1 ± 0.00

no compatibilizer (AB10FA10C0). The density increased progressively with rising fibre content, from 1.298 ± 0.07 g/cm³ for 2.5 wt.% (AB2.5FA10C0) to 1.714 ± 0.14 g/cm³ at 7.5 wt.% (AB7.5FA10C0), indicating effective reinforcement and minimal void formation. Composites containing PP-g-MAH also followed a similar trend. The highest density in treated samples was found for AB10FA10C3 (1.889 ± 0.02 g/cm³). Although slightly lower than its untreated counterpart, the reduction could be attributed to the lower matrix fraction due to additional PP-g-MAH. Nonetheless, the presence of a compatibilizer supported strong interfacial adhesion, as reflected by consistently high densities. However, FA10 and PP100 showed lower densities of 1.076 ± 0.02 g/cm³ and 0.90 ± 0.01 g/cm³, respectively, confirming the densifying effect of abaca fibre. The results demonstrated that abaca significantly enhanced the composite density, particularly at higher fibre contents, due to its higher intrinsic density and better compaction of the fibre within the matrix. Since density and specific density obtained the similar results and greater than 1 indicated composite is denser than water and will sink. This enabled a clearer comparison of mass–property relationships, thereby supporting the evaluation of the functional advantage offered by the hybrid composite system.

Across all composite formulations, the absorption remained low, ranging from 0.0% to 0.107%, indicating the good moisture resistance of the system. Among untreated samples, absorption was nearly constant at around 0.101%–0.102%, regardless of fibre content. This stability suggested that abaca's naturally dense structure and smoother surface limited water penetration, even without a PP-g-MAH. Treated composites containing PP-g-MAH exhibited similarly low water absorption. AB5.0FA10C2 recorded the lowest value of 0.0 ± 0.02 %, while the highest among treated samples was 0.107 ± 0.02 % for AB10FA10C3. The presence of PP-g-MAH likely improved fibre–matrix adhesion, reducing the number of microvoids and interfacial gaps that could allow water ingress. The composite only FA10 absorbed 0.103%, while neat polypropylene (PP100) showed a minimal uptake of 0.1%, consistent with its hydrophobic nature. The results confirmed that abaca-based composites were the most water-resistant among the fibre systems investigated, and a compatibilizer further stabilized moisture behavior.

For untreated composites, the void content remained relatively low and consistent at lower fibre loadings, 0.15 ± 0.06 % for AB2.5FA10C0, 0.16 ± 0.03% for AB5.0FA10C0 and 0.16 ± 0.07 for AB7.5FA10C0. However, a sharp increase was observed at higher fibre content, with AB10FA10C0 reaching 0.32 ± 0.04 %, likely due to fibre clustering and limited resin flow at elevated reinforcement levels. Similar behavior was noted in compatibilized composites. The void content for AB2.5FA10C2 and AB5.0FA10C2 remained stable at 0.16 ± 0.03 %, indicating effective matrix bonding and compaction. However, at higher loadings, AB7.5FA10C3 and AB10FA10C3 showed increased void contents of 0.31 ± 0.06 % and 0.32 ± 0.01 %, respectively. This suggested that while the compatibilizer improved interfacial bonding, excessive fibre still led to localized void formation. For comparison, the FA10 composite exhibited a void content of 0.18 ± 0.01 %, while the neat polypropylene (PP100) sample showed the lowest value of 0.10 ± 0.00 %, consistent with its homogeneous single-phase structure. The data confirmed that void content in abaca composites was strongly influenced by fibre loading, and that effective control was possible at or below 7.5 wt.% fibre content.

3.2 Mechanical Properties

The mechanical performance of abaca fibre-reinforced PP composites with FA filler was evaluated under standard test conditions, and experimental values obtained are represented in Table 3.

3.2.1 Tensile Properties

The tensile behavior of abaca fibre-reinforced PP composites incorporating 10 wt.% FA and varying compatibilizer (PP-g-MAH) content is presented through stress-strain curves (Fig. 3) and load-displacement profiles (Fig.4). The incorporation of abaca fibres significantly enhanced the tensile properties of the composites relative to neat polypropylene (PP100) and FA-only formulations (FA10). Neat PP100 exhibited the highest elongation but the lowest tensile strength (24.71 ± 0.30 MPa), reflecting its ductile nature. The FA10 composite showed slightly improved strength (26.27 ± 0.44 MPa) but reduced strain, indicating a more brittle behavior due to rigid filler inclusion[5,14, 16,17].

Untreated composites (AB7.5FA10C0) exhibited an increasing trend in tensile strength and modulus

Table 3 — Mechanical properties of abaca fibre-reinforced composites with and without compatibilizer: Mean and Standard Deviations (SD)

Fabricated Composites	Tensile Strength ± SD,MPa	Tensile Modulus ± SD, MPa	Flexural Strength ± SD,MPa	Flexural Modulus ± SD, MPa	Impact Strength ± SD, J/m	Shore D Hardness ± SD
AB2.5FA10C0	34.553 ± 0.87	1889.212 ± 0.20	39.353 ± 0.12	2532.333 ± 0.46	49.00 ± 0.03	60.00 ± 0.43
AB5.0FA10C0	35.234 ± 0.59	1943.483 ± 0.15	40.925 ± 0.43	2600.666 ± 0.47	52.34 ± 0.08	62.33 ± 0.11
AB7.5FA10C0	36.187 ± 0.11	2034.750 ±0.14	44.656 ± 0.59	2870.108 ± 0.60	54.00 ± 0.10	63.67 ± 0.11
AB10FA10C0	35.234 ± 0.49	1943.483 ± 0.15	43.860 ± 0.50	2802.503 ± 0.43	57.67 ± 0.15	63.67 ± 0.05
AB2.5FA10C2	37.605 ± 0.21	2050.261 ± 0.79	39.413 ± 0.22	2581.666 ± 0.11	45.67 ± 0.06	61.67 ± 0.40
AB5.0FA10C2	37.931 ± 0.28	2058.463 ± 0.11	40.307 ± 0.51	2597.333 ± 0.10	46.00 ± 0.04	63.67 ± 0.11
AB7.5FA10C3	38.177 ± 0.43	2223.054 ± 0.14	42.950 ± 0.44	2735.333 ± 0.10	58.67 ± 0.27	65.67 ± 0.05
AB10FA10C3	38.095 ± 0.66	2190.827 ± 0.21	44.940 ± 0.49	2933.523 ± 0.25	50.34 ± 0.09	64.00 ± 0.17
FA10	26.269 ± 0.44	1444.265 ± 0.57	37.665 ± 0.38	2297.050 ± 0.16	34.37 ± 0.07	60.67 ± 0.05
PP100	24.710 ± 0.30	1353.653 ± 0.44	35.325 ± 0.26	2124.070 ± 0.12	26.73 ± 0.06	55.00 ± 0.17

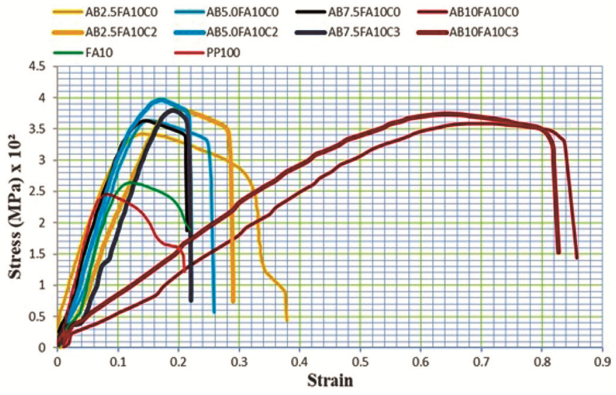

Fig. 3 — Stress-Strain Curve for Fabricated Composites

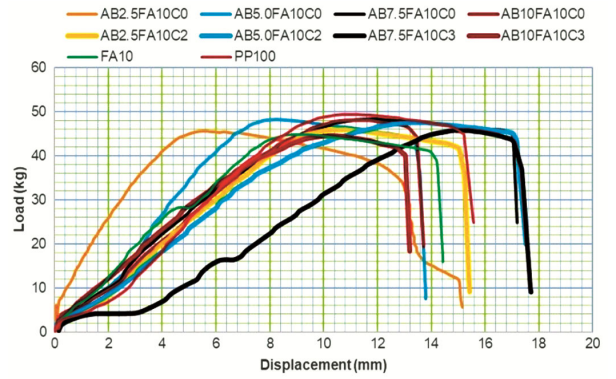

Fig. 4 — Load-displacement Curve for Fabricated Composites

Flexural Properties

with fibre loading up to 7.5 wt.%, peaking at 36.187 ± 0.11 MPa and 2034.750 ± 0.14 MPa, respectively. However, at 10 wt.% fibre (AB10FA10C0), a marginal reduction in tensile strength (35.234 ± 0.49 MPa) was observed, likely attributed to fibre agglomeration and increased void formation, which disrupted stress transfer[2,4,5,8].

Compatibilized composites (AB7.5FA10C3 and AB10FA10C3) exhibited superior tensile performance due to improved interfacial bonding facilitated by PP-g-MAH[12,13]. The sample AB7.5FA10C3 showed the highest tensile strength (38.177 ± 0.43 MPa) and modulus (2223.054 ± 0.14 MPa), indicating optimal fibre dispersion and stress transfer efficiency. Stress-strain profiles revealed improved ductility in compatibilized systems, suggesting enhanced fibre–matrix adhesion and reduced premature failure. Load-displacement curves further confirmed that compatibilized composites, especially AB5.0FA10C2 and AB7.5FA10C3, sustained higher loads and longer deformation paths before fracture, indicative of improved toughness and load-bearing capacity. However, the uncompatibilized high-fibre sample AB10FA10C0 showed earlier failure, highlighting the adverse effect of poor interfacial adhesion at higher reinforcement levels.

The present results align well with recent literature. Prior studies reported that FA improves stiffness but may reduce ductility when bonding is insufficient, explaining the trend in FA10 and AB10FA10C0[17]. Other works demonstrated that PP-g-MAH enhances fibre–matrix adhesion, consistent with the performance of AB7.5FA10C3[18]. Additionally, research highlighted that balanced tensile behavior requires optimal fibre loading and adequate interfacial adhesion, corroborating the trends observed here[2].

Although composites are typically designed to improve specific strength, the simultaneous use of FA and AB can reduce strain-at-break because FA stiffens the matrix and restricts deformation. This limits the effectiveness of AB fibres at higher loading. Nonetheless, FA offers additional benefits including slightly increased density, improved thermal stability, and cost efficiency which justify its inclusion in supporting sustainable composite formulations.

The tensile results demonstrated that a moderate fibre content (5–7.5 wt.%) combined with 2–3 wt.%

PP-g-MAH compatibilizer achieved the best balance of tensile strength, stiffness, and ductility. These findings support the role of compatibilization in enhancing the mechanical performance of natural fibre-reinforced PP composites, particularly by mitigating interfacial defects and improving load transfer efficiency.

3.2.2 Flexural Properties

The flexural strength and modulus values for Abaca fibre-reinforced PP composites are presented in Table 3. The results indicated that fibre reinforcement improved flexural performance over the control samples, and that the addition of PP-g-MAH further enhanced stiffness and strength, particularly at higher fibre loadings. For untreated composites, the highest flexural strength was observed for AB7.5FA10C0 (44.656 ± 0.59 MPa), followed by AB10FA10C0 (43.860 ± 0.50 MPa). Strength increased consistently from AB2.5FA10C0 (39.353 ± 0.12 MPa) through to 7.5 wt.% fibre, indicating enhanced load-bearing capacity with increasing reinforcement. However, the slight drop at 10 wt.% suggested the onset of fibre clustering or limited resin flow.

A similar trend was observed in flexural modulus, which increased from 2532.333 ± 0.46 MPa to 2870.108± 0.60 MPa in untreated composites, then slightly dropped at 10 wt.%. Compatibilized composites showed comparable or better performance. AB10FA10C3 exhibited the highest flexural modulus (2933.523 ± 0.25 MPa) and strength (44.940 ± 0.49 MPa), confirming that the compatibilizer improved interfacial adhesion and matrix continuity. However, AB5.0FA10C2 and AB2.5FA10C2 did not show significant improvements over their untreated counterparts, suggesting that the compatibilizer was most effective at higher fibre content. FA10 and PP100 exhibited the lowest flexural properties, with strength values of 37.665 ± 0.38 MPa and 35.325 ± 0.26 MPa, and modulus values of 2297.050 ± 0.16 MPa and 2124.070 ± 0.12 MPa, respectively. The results confirmed that Abaca fibre, particularly when used with a compatibilizer at 7.5–10 wt.%, appreciably enhanced both strength and stiffness under flexural loading.

The flexural behaviour observed in this study aligns well with recent reports on natural fibre–reinforced PP hybrids. Increasing fibre loading has been shown to improve stress transfer and bending stiffness, consistent with the rise in flexural strength from AB2.5FA10C0 to AB7.5FA10C0[24]. The beneficial role of PP-g-MAH in strengthening fibre–matrix adhesion has also been widely reported[25], supporting the superior performance of AB10FA10C3. Further, earlier studies noted that excessive fibre addition can lead to agglomeration and hinder resin flow[26], corresponding with the slight decline observed at 10 wt.% in both untreated and compatibilized composites. These similarities reinforce the reliability and scientific validity of the present flexural trends.

3.2.3 Impact Properties

The impact strength results for abaca fibre-reinforced composites are summarized in Table 3. The incorporation of abaca fibresignificantly enhanced the impact resistance of the PP matrix, with performance influenced by both fibre content and the compatibilizer. Among untreated composites, impact strength increased steadily with fibre loading, reaching 57.67 ± 0.15 J/m for AB10FA10C0, the highest among untreated groups. This improvement was attributed to the energy absorption mechanisms enabled by fibre pull-out and microcrack deflection during fracture. Composites with 2.5–7.5 wt.% fibre (AB2.5FA10C0 to AB7.5FA10C0) also showed a consistent upward trend, from 49 ± 0.03 J/m to 54 ± 0.10 J/m.

In compatibilized composites, the highest impact strength (58.67 ± 0.27 J/m) was observed for AB7.5FA10C3, outperforming even the untreated AB10FA10C0 sample. This result highlighted the positive role of PP-g-MAH compatibilizer in improving interfacial bonding and energy dissipation. However, AB10FA10C3 showed a lower value (50.34 ± 0.09 J/m), possibly due to overloading effects, fibre clustering, or void formation at higher fibre and compatibilizer content. AB2.5FA10C2 and AB5.0FA10C2 exhibited slightly reduced impact strengths (45.67 ± 0.06 J/m and 46 ± 0.04 J/m, respectively) compared to their untreated counterparts, suggesting that the compatibilizer may not be as effective at lower fibre contents. This is consistent with the literature, where natural fibres contribute to microcrack deflection and energy dissipation during impact loading[26]. FA10 control recorded 34.37 ± 0.07 J/m, while neat polypropylene (PP100) showed the lowest value (26.73 ± 0.06 J/m), underscoring the toughening effect of abaca fibre reinforcement. The results confirmed that 7.5–10 wt.% abaca fibre, especially with the compatibilizer, provided the most favorable impact resistance among the tested formulations.

The observed impact trends are consistent with previous studies. Natural fibres improved impact resistance primarily through fibre pull-out and microcrack deflection, corroborating the enhanced toughness observed in AB7.5FA10C3 and AB10FA10C0[18]. Similarly, PP-g-MAH improves interfacial adhesion and promotes better energy dissipation, supporting the superior performance of compatibilized composites in the present work[2]. Excessive fibre loading may lead to fibre clustering and void formation, which is consistent with the reduced impact strength observed in AB10FA10C3[19]. These parallels results confirmed that the impact behavior of the developed composites follows the established mechanisms reported in the literature.

3.2.4 Hardness

The Shore D hardness values of the fabricated composites are presented in Table 3. As observed, the hardness increased with fibre loading and the incorporation of compatibilizer. The highest value without PP-g-MAH (63.67 ± 0.11) was observed at 7.5–10 wt.% fibre, indicating improved stiffness and reduced polymer chain mobility due to the fibre presence. Compatibilized composites AB7.5FA10C3 (65.67 ± 0.05) were recorded with further improvement in hardness, indicating improved surface rigidity due to enhanced fibre–matrix bonding. FA10 showed an increase in hardness (60.67 ± 0.05), demonstrating the rigid nature of FA, which restricts surface deformation. PP100 exhibited the lowest hardness value (55 ± 0.17), attributed to its soft, ductile nature and lack of reinforcement. The results confirmed that both fibre loading and compatibilizer addition contribute positively to surface hardness, with 7.5 wt.% abaca and 10 wt.% FA being the most effective composition.

3.3 Morphological Analysis

FESEM analysis of fractured tensile specimens was conducted to evaluate the microstructural characteristics of abaca fibre-reinforced PP composites with 10 wt.% FA and varying fibre and compatibilizer contents.

As shown in Fig. 5(a-d), composites without compatibilizer revealed progressive microstructural

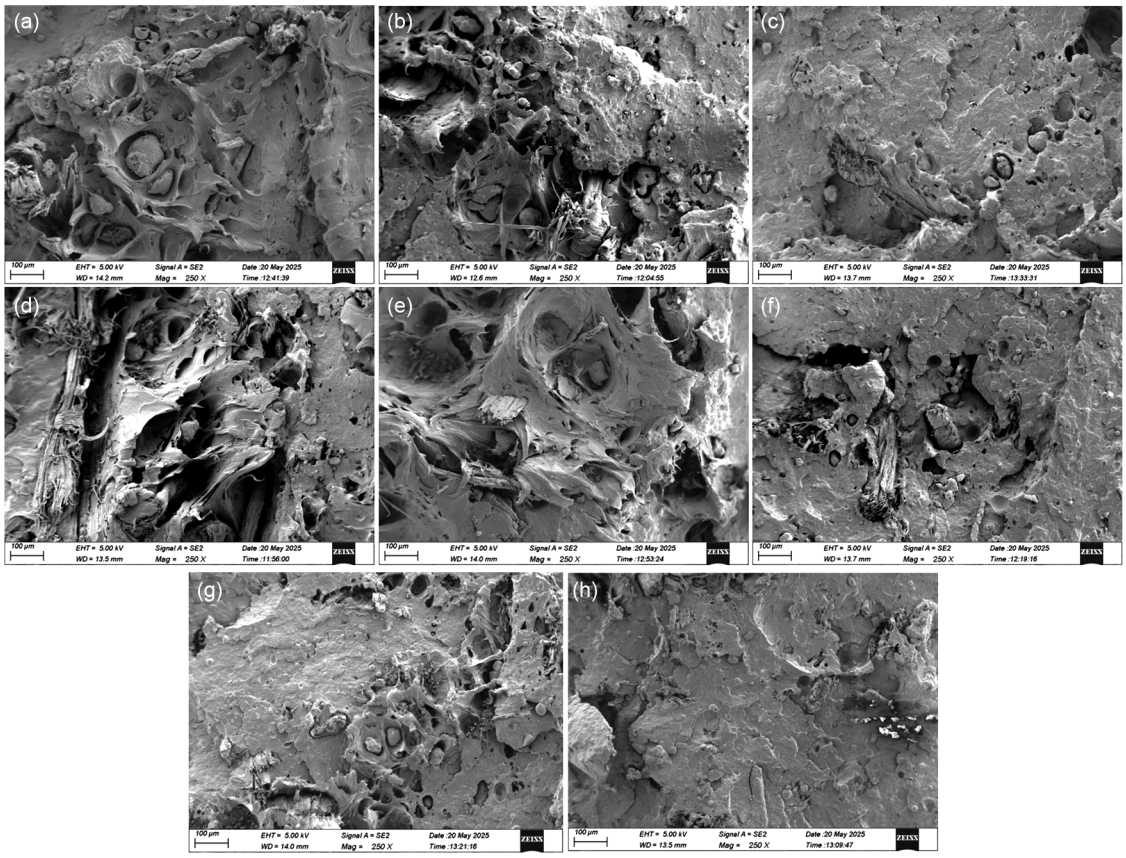

Fig. 5 — FESEM Analysis, (a) AB2.5FA10C0, (b) AB5.0FA10C0, (c) AB7.5FA10C0, (d) AB10FA10C0, (e) AB2.5FA10C2, (f) AB5.0FA10C2, (g) AB7.5FA10C3, and (h) AB10FA10C3

development with increasing fibre content. AB2.5FA10C0 displayed a smooth matrix with sparse fibre pull-out and poor interfacial engagement, indicating limited reinforcement and a matrix-dominated fracture. AB5.0FA10C0 exhibited improved fibre dispersion, embedded fibre ends, and matrix tearing, suggesting better stress transfer and interfacial bonding. AB7.5FA10C0 presented the most favorable morphology, dense fracture surfaces with embedded and fractured fibres, consistent with peak mechanical performance. AB10FA10C0 showed signs of fibre agglomeration, voids, and detachment zones, indicating compromised bonding and explaining the slight reduction in strength at higher fibre content.

Similarly, as shown in Fig. 5(e-h), the addition of PP-g-MAH significantly enhanced the interfacial integrity and microstructural cohesion. AB2.5FA10C2 exhibited reduced voids and better matrix wetting, even at low fibre content, confirming improved stress transfer through compatibilization. AB5.0FA10C2 showed minor interfacial gaps and void clusters, suggesting only partial compatibilizer effectiveness at this composition. AB7.5FA10C3 revealed excellent morphological features, strong matrix continuity, minimal voids, and fractured fibre fragments corresponding to the highest flexural and impact strengths. AB10FA10C3, while compatibilized, displayed renewed signs of fibre clustering and porosity, implying saturation of the compatibilizer's effectiveness at excessive fibre loadings.

FESEM observations confirmed that 7.5 wt.% abaca fibre, especially with 3 wt.% PP-g-MAH offered the most optimal fibre–matrix interaction and minimal structural defects. At 10 wt.%, both treated and untreated composites exhibited interfacial degradation due to fibre agglomeration and limited matrix flow. These findings aligned well with the mechanical results, reinforcing the critical role of microstructural integrity in hybrid composite performance.

4 Conclusion

This research comprehensively investigated the mechanical, physical, and morphological properties of abaca fibre, fly ash, and polypropylene composites, with varying fibre, filler, and compatibilizer contents.

Mechanical performance significantly improved with increasing abaca fibre content. In uncompatibilized composites, tensile strength increased by 39.8–46.4%,while flexural strength rose by 11.4–26.4%. Impact strength reached a maximum improvement of 115.7%at 10 wt.% fibre. The addition of 3 wt.% PP-g-MAH further enhanced these properties, AB7.5FA10C3 exhibited the highest tensile strength (+54.6%), tensile modulus (+64.2%), and impact strength (+119.6%). Flexural strength and modulus were maximized in AB10FA10C3, (+27.2% and +38.1%respectively). These results confirmed that the compatibilizer strengthened fibre–matrix adhesion, enabling efficient stress transfer and improved load-bearing capacity. Shore D hardness also followed this trend, showing an improvement of 9.09–19.4%, reflecting enhanced surface integrity due to effective reinforcement and interfacial compatibility. Physical properties aligned with these trends. Composite density increased proportionally with fibre content, increasing from 44.2% to 113.6% for uncompatibilzed composites, and from 41.8-109.9% for compatibilized composites. This indicated effective incorporation of high-density FA and abaca fibre into the matrix. Water absorption remained low (0.1%) across all samples, indicating minimal moisture uptake, though slightly higher values were seen in AB10FA10C3 (7%) due to higher loading. Void content increased at higher fibre loadings – reaching 22% in both AB10FA10C0 and AB10FA10C3, reflecting challenges in processing and fibre dispersion beyond the optimal threshold. FESEM analysis supported the mechanical and physical findings. Uncompatibilized composites (e.g., AB10FA10C0) showed fibre agglomeration, matrix cracks, and voids, explaining the observed drop in ductility and strain. However, AB7.5FA10C3 displayed well-dispersed fibres, strong fibre–matrix bonding, and minimal porosity, justifying its superior mechanical and hardness performance. However, at 10 wt.% fibre, even with compatibilizer, fibre crowding and interfacial degradation re-emerged.In conclusion, the optimal composite formulation was achieved at 7.5–10 wt.% abaca fibre, 10 wt.% FA, and 3 wt.% PP-g-MAH, which balanced high mechanical strength, good physical integrity, and strong interfacial bonding. These findings underscore the synergy between reinforcement, compatibilization, and microstructure clearly demonstrated. Abaca–PP composite without FA or compatibilizer was not evaluated in this study, future inclusion of abaca–PP would provide a more comprehensive understanding of the individual contribution of abaca reinforcement to the overall composite performance. Although PP is not fully biodegradable and the developed composite cannot be considered 100% eco-friendly, the use of abaca fibre

and FA contributes to supportive sustainable material technology by reducing synthetic content and valorizing industrial/agro-waste. These results validate the role of abaca fibre/FA/PP composites for lightweight, performance-oriented, and sustainability-enhanced composite applications.

Acknowledgments

The authors express their sincere appreciation to the Institute of Chemical Technology, Veermata Jijabai Technological Institute, and Indian Institute of Technology, Mumbai, for providing laboratory facilities and technical support throughout this work. The study was independently conducted and did not benefit from any financial assistance from governmental, private, or non-profit organizations.

References

1 Pickering KL, Aruan Efendy MG& Le TM,*Compos Part A: Appl Sci Manuf*, 83 (2016) 98.
2 Karthik K, Rajamanikkam R K, Venkatesan E P, Bishwakarma S, Krishnaiah R, Saleel C A, Soudagar M E M, Kalam M A, Ali M M &Bashir M N, *Chin J Anal Chem*, 52 (7) (2024) 100415.
3 Cai M, Takagi H, Nakagaito AN, Katoh M, Ueki T, Waterhouse GIN& Li Y,*Ind Crops Prod*, 65 (2015) 27.
4 Sinha AK, Bhattacharya S& Narang HK, *J Mater Sci*, 56 (2021) 4569.
5 Rajkumar G, Sathishkumar G K, Srinivasan K, Karpagam R, Dhivya V, Sakthipandi K & Mohamed Akheel M, *J NatFibres*, 19 (13) (2021) 6534.
6 Delicano JA,*Compos Interfaces*, 25 (12) (2018) 1039.
7 Punyamurthy R, Sampathkumar D, Ranganagowda RP, Bennehalli B, Badyankal P& Venkateshappa SC,*Ciênc Tecnol Mater*, 26 (2) (2014) 142.
8 Dabet A, Homma H & Homma H, *Mech Eng J*, 5 (5) (2018) 78.
9 Venkatasubramanian H& Raghuraman S,*J Eng Sci Technol*,10 (8) (2015) 958.
10 Suriani MJ, Ilyas RA, Zuhri MYM, Khalina A, Sultan MTH, Sapuan SM, Ruzaidi CM, Wan FN, Zulkifli F, Harussani MM, Azman MA&Radzi FSM, *Polymers*, 13 (20) (2021) 3514.
11 Jagatheesan K & Satheeshkumar T, *Indian J Fibre Text Res*, 49(2) (2024) 237.
12 González-López ME, Robledo-Ortíz JR, Manríquez-González R, Silva-Guzmán JA & Pérez-Fonseca A, *Compos Interfaces*, 25 (5–7) (2018) 515.
13 Azizli MJ, Barghamadi M& Rezaeeparto K, *J Polym Res*, 29 (2022) 322.
14 Mathapati M, Amate K, Durga Prasad C, Jayavardhana ML& Hemanth Raju T,*Materials Today: Proceedings*, 50 (5) (2022) 1535.
15 Maurya AK, Gogoi R& Manik G,*Poly Compos*, 43 (2) (2021) 1060.
16 Pal T, Pramanik S, Verma KD, Naqvi SZ, Manna PK& Kar KK,*Handbook of Fly Ash(Butterworth-Heinemann)*, 2022, 243.
17 Alghamdi M N,*Poly*, 14 (14) (2022) 2913.
18 Kumar P, Gupta H S, Singh M, Chaudhari A S, Maurya A K, Manik G, *Chem Eur J*, 31 (2) (2025) 202402393.
19 Bilal H, Gao X, Cavaleri L, Khan A, Ren M, *J Compos Sci*, 8 (11) (2024), 456.
20 Bledzki AK, Franciszczak P, Osman Z& Elbadawi M,*Ind 1*. R, Ferrandiz S, *Procedia Manuf*, 13 (2017) 321-326.
21 Rosamah E, Hossain MdS, Abdul Khalil HPS, Wan Nadirah WO, Dungani R, Nur Amiranajwa AS& Mohd Omar AK,*Adv Compos Mater*, 26 (3) (2016) 259.
22 Mirbagheri J, Tajvidi M, Hermanson JC& Ghasemi I,*J Appl Polym Sci*, 105 (2007) 3054.
23 Mulenga TK, Rangappa SM & Siengchin S,*Express Polym Lett*, 19 (5) (2025) 470.
24 Rosamah E, Hossain MdS, Abdul Khalil HPS, Wan Nadirah WO, Dungani R, Nur Amiranajwa AS& Mohd Omar AK,*Adv Compos Mater*, 26 (3) (2016) 259.
25 Mirbagheri J, Tajvidi M, Hermanson JC& Ghasemi I,*J Appl Polym Sci*, 105 (2007) 3054.
26 Mulenga TK, Rangappa SM & Siengchin S,*Express Polym Lett*, 19 (5) (2025) 470.